Mol. Cells *30*, 551-556, December 31, 2010
DOI/10.1007/s10059-010-0152-6

Molecules and Cells

Solution Structures and Molecular Interactions of Selective Melanocortin Receptor Antagonists

Chul-Jin Lee, Ji-Hye Yun, Sung-Kil Lim[1], and Weontae Lee*

The solution structures and inter-molecular interaction of the cyclic melanocortin antagonists SHU9119, JKC363, HS014, and HS024 with receptor molecules have been determined by NMR spectroscopy and molecular modeling. While SHU9119 is known as a nonselective antagonist, JKC363, HS014, and HS024 are selective for the melanocortin subtype-4 receptor (MC4R) involved in modulation of food intake. Data from NMR and molecular dynamics suggest that the conformation of the Trp9 sidechain in the three MC4R-selective antagonists is quite different from that of SHU9119. This result strongly supports the concept that the spatial orientation of the hydrophobic aromatic residue is more important for determining selectivity than the presence of a basic, ''arginine-like'' moiety responsible for biological activity. We propose that the conformation of hydrophobic residues of MCR antagonists is critical for receptor-specific selectivity.

INTRODUCTION

The melanocortin receptor system consists of five receptor subtypes (MC1R-MC5R) and belongs to the superfamily of G-protein coupled receptors. These melanocortin receptors play an important role in skin pigmentation (Mountjoy et al., 1992), adrenocortical function (Mountjoy et al., 1992), energy homeostasis (Butler et al., 2000; Chen et al., 2000), feeding behavior (Fan et al., 1997; Huszar et al., 1997), sexual function (Wessells et al., 2003), and exocrine gland function. The receptor MC4R, expressed predominantly in the brain, is a promising obesity drug target. The cyclic peptides SHU9119, JKC363, HS014, and HS024 are potent antagonists of the melanocortin receptors. While SHU9119 is a non-selective antagonist, JKC363, HS014, and HS024 are selective antagonists of MC4R. The antagonist HS014 is potent, selective for the MC4R ligand (K_i = 3.2 nM), and has 17-fold selectivity for MC4R over MC3R. The antagonist JKC363 is three times more potent than HS014 for MC4R. The antagonist HS024 has about 20-fold selectivity for MC4R over MC3R and very high affinity (K_i = 0.29 nM) for MC4R (Chai et al., 2003; Kask et al., 1998). The nonselective cyclic MC4R peptide antagonist SHU9119 has potencies to increase food intake similar to HS024. However, because SHU9119 does not have receptor selectivity, it has many serious side effects. Therefore, to develop a potent MC4R antagonist as an effective treatment for increasing feeding, the selectivity of these cyclic peptides must be developed. Two-dimensional nuclear magnetic resonance (2D NMR) spectroscopy was used to determine the solution structures of the cyclic melanocortin agonists SHU9119, JKC363, HS014, and HS024.

Previous studies have reported the presence of a positively charged arginine residue located opposite of the hydrophobic group of the core sequence and involved in charge-charge interactions with the negatively charged residues in the transmembrane helix 2 and 3 (TMH2 and TMH3) regions of the receptors. In this study, we found an important structural difference between the nonselective SHU9119 and the other selective melanocyte-stimulating hormone (MSH) antagonists JKC363, HS014, and HS024. Although the spatial dispositions of the aromatic groups are similar, the backbone shape of JKC363, HS014, and HS024 differs from that of SHU9119. Additionally, the Arg8 sidechains of the MC4R-selective antagonists JKC363, HS014, and HS024 have an orientation opposite of that in SHU9119. This result suggests that the Arg8 residues of these selective cyclic peptides are not critical for binding to MC4R. To test this hypothesis and understand the molecular interactions between MCRs and these antagonists, we performed automated docking studies and molecular dynamics simulations. Our goal in this study was to create information to use for a structural basis for the design of selective antagonists for the melanocortin receptors.

MATERIALS AND METHODS

Peptide synthesis and NMR sample preparation

Four cyclic peptides, SHU9119, JKC363, HS014, and HS024 were synthesized by Anygen Co. (Korea). The peptides were determined greater than 98% pure by high-pressure liquid chromatography and mass spectrometry. For NMR experiments, all peptides were dissolved at 3 to 5 mM in 90% H_2O/10% D_2O or 99.9% D_2O with 25 mM sodium phosphate at pH 6.5.

NMR experiments

NMR experiments were performed on a Bruker DRX-500 spectrometer in quadrature detection mode using a triple-resonance

Department of Biochemistry, College of Life Science and Biotechnology, Yonsei University, Seoul 120-749, Korea, [1]Department of Internal Medicine, College of Medicine, Yonsei University, Seoul 120-749, Korea
*Correspondence: wlee@spin.yonsei.ac.kr

Received July 19, 2010; revised September 11, 2010; accepted September 13, 2010; published online November 23, 2010

Keywords: antagonist, homology modeling, melanocortin, melanocortin receptor, nuclear magnetic resonance

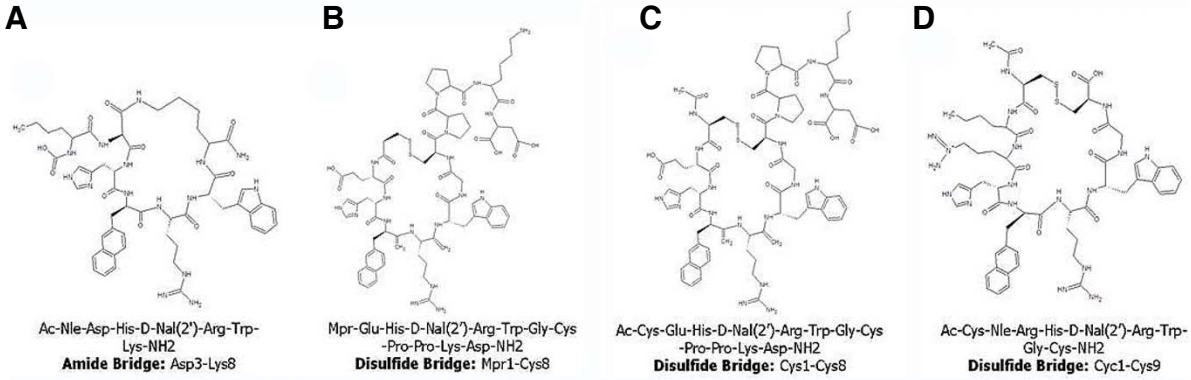

Fig. 1. The peptides SHU9119 (A), JKC363 (B), HS014 (C), and HS024 (D) are schematically represented. Nle indicates norleucine; Mpr, β-mercaptopropionate; and *D*Nal, β-(2-naphthyl)-*D*-alanine.

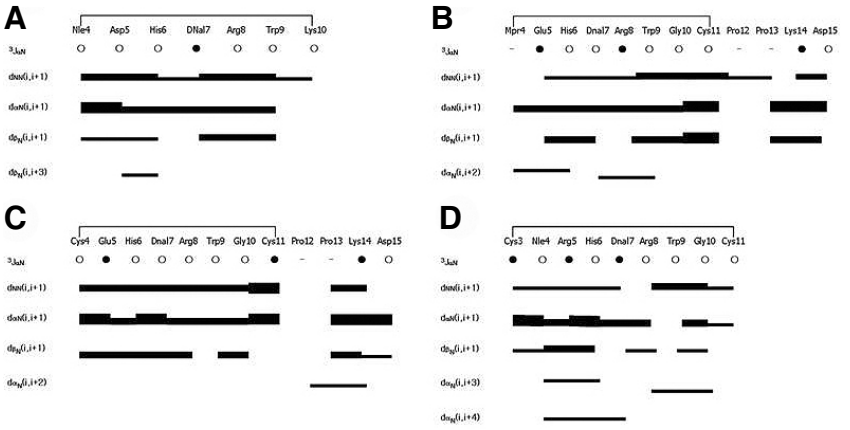

Fig. 2. The NMR data at pH 6.5 and 5°C for SHU9119 (A), JKC363 (B), HS014 (C), and HS024 (D) are summarized. The sequential and short-range NOE contacts are shown. For the backbone vicinal coupling constants, the close circle indicates $^3J_{NH\alpha} < 6$ Hz.

probe equipped with an actively shielded pulsed field gradient (PFG) coil. All two-dimensional data were collected at 5°C. Data were processed using NMRPipe/NMRDraw (Biosym/Molecular Simulations, Inc.) or XWIN-NMR (Bruker Instruments) software on a Silicon Graphics Indigo^2 workstation and analyzed using the Sparky 3.95 program (T. D. Goddard and D. G. Kneller, UCSF).

Experimental constraints and structure calculations

The solution structures were calculated by the distance geometry and dynamic simulated annealing (SA) procedures with the CNS 1.1 program (Yale University). The target functions for molecular dynamics and energy minimization were a covalent structure, van der Waals repulsion, NOE, and torsion angle constraint. By basing the cross peak intensities on the NOESY/ROESY spectra with mixing times of 150 to 600 ms, the distance constraints were classified into three distance categories: strong (0.18 to 0.27 nm), medium (0.18 to 0.33 nm), and weak (0.18 to 0.5 nm). The backbone dihedral restraints inferred from the $^3J_{HN\alpha}$ coupling constants were -55 ± 45° for $^3J_{HN\alpha}$ less than 6 Hz and -120 ± 50° for $^3J_{HN\alpha}$ greater than 8 Hz. Final structures are displayed using the Pymol program (DeLano Scientific LLC.).

Molecular modeling of MSH analogues and receptor complexes

Automated docking with the Autodock program (SCRIPPS) was performed to find optimum binding mode of the ligand molecules (Goodsell et al., 1996) using Lamarckian genetic algorithm on grids of 0.375 Å resolution. From the Autodock scoring function, we selected the sidechain orientation with the best score during all the 300 runs performed with this program. To observe the energetically favored state, molecular dynamics simulations for the selected ligand-receptor complex model were performed using Gromacs force field (Lee et al., 2009; Lindahl et al., 2001). To mimic the lipid membrane environments, dynamics simulations were executed using a pre-equilibrated palmitoyl oleoylphosphatidyl ethanolamine (POPE) lipid bilayer solvated in SPC water (Kollman, 1993). Lipids and water molecules were removed to insert the receptor molecule into the cavity. Each structure was equilibrated for 20 ps and subsequently subjected to a 1-ns dynamics at 300K, with a step size of 1 fs to explore different peptide and receptor conformations.

RESULTS

Structural comparison of MSH analogues

Backbone sequential assignments were completed by following $d_{\alpha N}$ (i, I+1) NOE connectivity in the NOESY spectrum (Wuthrich, 1996). The sidechain proton resonances were easily identified by TOCSY connectivity. All of the sequential and short-range NOE connectivity and $^3J_{HN\alpha}$ coupling constants for MSH analogues were identified (Fig. 2). The three peptides JKC363, HS014, and HS024 were cyclized by disulfide bond and had interresidue NOEs between ring protons of *D*Nal7 and sidechain protons of Arg8 detected. However, those NOEs were not observed with SHU9119, which was cyclized by lactam bridge. These data are consistent with the suppositions in Fig. 4 that the conformation of the core sequence of SHU9119 con-

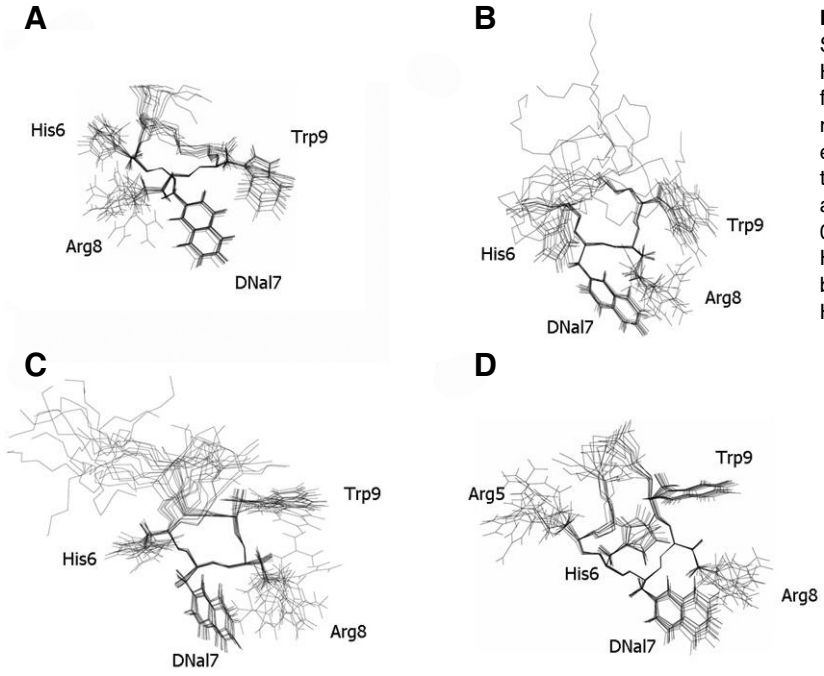

Fig. 3. The final simulated annealing structures of SHU9119 (A), JKC363 (B), HS014 (C), and HS024 (D) displays the superposition of the 12 final $<SA>_k$ structures for each over the energy minimized average structures. The total number of experimental restraints used to generate the structures and the backbone RMSD values were 174 and 0.59 ± 0.22 Å for SHU9119, 139 and 0.31 ± 0.13 Å for JKC363, 193 and 0.49 ± 0.20 Å for HS014, and 157 and 0.41 ± 0.14 Å for HS024. All backbone atoms are superimposed for residues His6 - Trp9.

Table 1. Summary of NOE distance restraints and structural statistics for MSH antagonists

		SHU9119	JKC363	HS014	HS024
NOE distance restraints	Intracresidue	125	72	86	78
	Sequentaial	18	25	33	21
	Long	31	42	74	58
	Total	174	139	193	157
	Restraints/ residue	25	11	16	13
Rmsd from ideal geometry (Å)	Bond (Å)	0.0023	0.0031	0.0015	0.0032
	Angle (deg)	0.41	0.47	0.34	0.40
	Impr (deg)	0.18	0.20	0.11	0.35
Energies (Kcal · mol^{-1})	NOE	3.67	3.73	3.65	3.64
	Bond	0.84	1.83	0.47	1.73
	Angle	8.42	8.20	6.58	7.60
	Impr	0.34	0.50	0.18	2.01
	vdW	0.26	0.41	0.10	0.22
	Total	13.53	14.66	10.98	15.21
	Lennard-Jones[a]	-16.71	-41.3	-24.92	-19.26
Atomic rmsd (Å) from average for backbone atoms (N, C^{α}, C') ideal geometry	All res.	0.83	1.24	1.39	0.72
Atomic rmsd (Å) from average for all non hydrogen atoms	All res.	1.23	1.71	2.04	1.46

[a]Lennard-Jones is the Lennard ± Jones/van der Waals potential calculated using CHARMm empirical energy function

siderably differs from that of JKC363, HS014, and HS024. For SHU9119, the NOEs between the ring protons of *D*Nal7 and sidechain protons of Nle4 were observed, suggesting that the sidechain protons of Nle4 are spatially adjacent to *D*Nal ring. The number and type of NOE distance restraints and other statistical data are summarized in Table 1. On average, 11 to 25 distance restraints per residue were available for structure determination. For each peptide, the 12 structures with the lowest restraint energies were used to represent structure. An ensemble of 50 DG conformers for each peptide served as the starting structures for dynamic simulated annealing calculations. The average structure was calculated from the geometrical average of structure coordinates and then subjected to restrained energy minimization (REM). Superposition of all $<SA>_k$ and $<SA>_{kr}$ structures is displayed in Fig. 3. The 12 lowest restraint energy structures of SHU9119, JKC363, HS014, and HS024 are illustrated as superimposed on the minimized mean structure of each peptide using the backbone heavy atoms of His6 through Trp9. The structures within the message sequence (His6, *D*Nal7, Arg8, and Trp9) were well defined. The backbone RMSD values were 0.59 ± 0.22 Å for SHU9119, 0.31 ± 0.13 Å for JKC363, 0.49 ± 0.20 Å for HS014, and 0.41 ± 0.14 Å for HS024.

By comparing the structures of SHU9119, JKC363, HS014, and HS024 (Fig. 4), we found that the orientation of Arg8 in JKC363, HS014, and HS024, the three peptides cyclized by a disulfide bond, is opposite of its orientation in SHU9119. As previously reported (Ying et al., 2003), SHU9119 has a reverse-turn structure (Lewis et al., 1973) that forms in the message sequence (His6, *D*Phe7/*D*Nal7, Arg8, and Trp9), and has Arg8 oriented to the opposite side of *D*Nal7 and Trp9. However, JKC363, HS014, and HS024 do not have the reverse-turn structure in message sequence, and Arg8 is oriented in the same direction as *D*Nal7. In these three peptides, the side chains of Arg8 and *D*Nal7 are located on the same side and the side chain protons of Arg8 are spatially closed to the *D*Nal ring, which is supported by NOEs between the ring protons of DNal7 and the sidechain protons of Arg8. The three peptides JKC363, HS014, and HS024, which were cyclized by a disulfide bond, have a similar conformation about the core residues. When

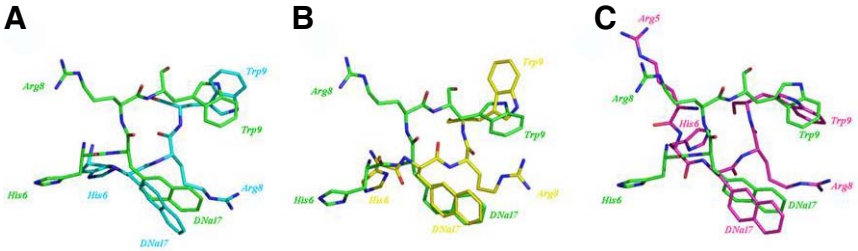

Fig. 4. The lowest restraint energy structures of SHU9119 with carbon atoms in green were compared with JKC363 with carbon atoms in cyan (A), HS014 with carbon atoms in yellow (B), and HS024 with carbon atoms in magenta (C).

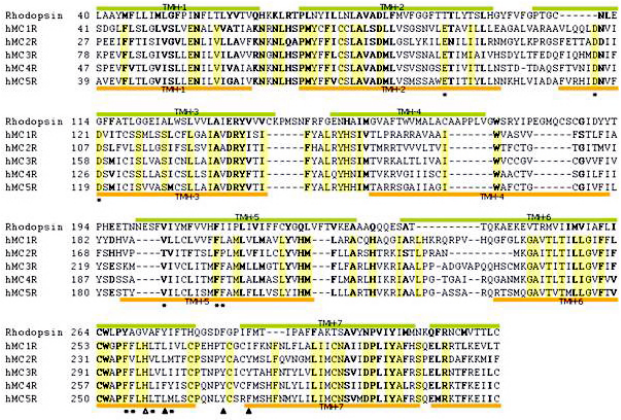

Fig. 5. The sequence of bovine rhodopsin was aligned with five human MCRs. Bold characters represent residues conserved in both bovine rhodopsin and MCRs. The green bars represent residues in α helices of bovine rhodopsin, and the orange bars represent residues from α helices of hMCRs. Residues that are identical across the five MCRs are yellow. Asterisks indicate residues anticipated to interact with MSH antagonists. The open triangle indicates His264 of MC4R that interacts with Trp9 of MC4R-selective antagonists. Closed triangles indicate Phe264 of MC4R and residues interacting with that phenylalanine.

SHU9119 is structurally aligned with the other three peptides JKC363, HS014, and HS024 (Fig. 4), the sidechain dispositions of most residues, except for Arg8, of message sequence are quite similar. When the sidechain orientations were compared, the Arg8 side chain of JKC363, HS014, and HS024 was oriented in the opposite direction of the *D*Nal7 and Trp9 aromatic rings. The unique orientation of Arg8 in JKC363, HS014, and HS024 differentiates their backbone shape from that of SHU9119. The Arg4 of HS024 was positioned on the same side with respect to Arg8 of SHU9119 (Fig. 4C), and so the Arg5 of HS024 could be involved in charge-charge interactions with the acidic residues on opposite side of the hydrophobic region.

Structure-function of MSH analogues

The center of the message sequence of peptides including SHU9119 has been reported to form a stable β-turn structure (Haskell-Luevano et al., 1996; Lee et al., 1998). Our NMR data indicate that the turn conformations of the central residues of JKC363, HS014, and HS024 appreciably differ from the β-turn structure of SHU9119. The cyclation of peptides is generally believed to increase the rigidity of the backbone, so that the cyclic MSH peptides bind to MCRs with more affinity than their linear counterparts (Lee et al., 1998). In view of structure-activity relationship, our results suggest that the various selectivities and potencies of the peptides result from structural differences. The 26 to 29 members of the rings of the three cyclic peptides JKC363, HS014, and HS024 create a larger ring than the 23 member ring of SHU9119. The increased ring size presumably results a more flexible peptide. Thus, larger rings might explain the lower affinity of the cyclic peptides JKC363, HS014, and HS024 compared to SHU9119. The peptide HS024 has about 10-fold more potency for MC4R than HS014 (K_i = 0.29 nM). We believe that the high affinity of HS024 is because Arg4 is positioned similarly to Arg8 of SHU9119. The Arg4 residue of HS024 is expected to be involved in charge-charge interactions with the acidic region of the ligand binding site similar to Arg8 of SHU9119.

Molecular interaction between MSH antagonist and MCR

We modeled the MCR-antagonist complexes to rationalize the ligand-receptor interaction on the molecular structure level. We selected coordinates of the bovine rhodopsin X-ray crystal structure (PDB code: 1f88) as a starting platform (Fig. 5). We performed an automated docking procedure to find the optimum binding mode of the ligand molecule and performed molecular dynamics simulations to observe the energetically favored state. The structural model of the JKC363/hMC4R complex shows that Arg8 and *D*Nal7 are located on the same side, the hydrophobic region of binding pocket (Fig. 6A). This result strongly supports the concept that the spatial orientation of the aromatic groups is more important than the presence of a basic "arginine-like" moiety. Although Trp9 of SHU9119 on MC4R interacts with Val193, Ile265, and Phe268 in TMH6 and TMH7, Trp9 of HS014 on MC4R only contacts His264 (Fig. 6B). This may be why HS014 can only bind MC4R since MC1R, MC3R, and MC5R do not have a positively charged residue that corresponds to His261 of MC4R. We also observed this unique interaction in the JKC363/MC4R complex.

During the MD simulation for MC4R, Phe264 had hydrophobic interactions with Tyr276 and Phe280 in TMH6-TMH7 exoloop, inducing the rotation of TMH6 and causing location of Phe261 inside the binding pocket. However, MC1R, MC3R, and MC5R have leucine residues corresponding to Phe267 in MC4R that are not bulky enough to interact with the hydrophobic residues in TMH6-TMH7, so that each TMH6 has insufficient rotation and His264 is not located inside the binding pocket. This leads us to postulate that the MC4R-specific selectivity of the cyclic peptides JKC363, HS014, and HS024 is due to the interaction between their Trp9 residues and the positively charged H264 of MC4R and to the docking of Arg4 of HS024 into MC4R that is located in acidic region of the ligand-binding

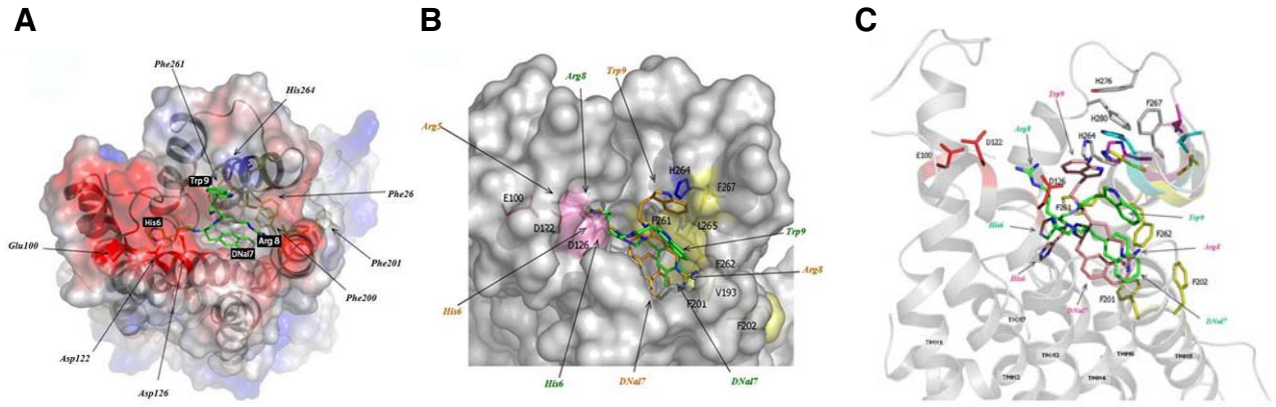

Fig. 6. The complex formed by MCR and MSH antagonist was molecularly modeled. Curvature and electrostatic potential surface of JKC363/MC4R complex is shown (A). The binding of SHU9119 (green) and HS024 (orange) to the putative binding pocket of human MC4R is illustrated (B), with yellow residues representing the hydrophobic region, pink residues representing the acidic region, and blue indicating the interaction of His264 with Trp9 of HS024. The binding modes of SHU9119 (green) and HS014 (pink) are compared (C), with yellow representing the residues involved in hydrophobic interactions, and red representing the residues involved in charge-charge interactions with the ligand. The residues corresponding to H264 and F267of MC4R are displayed with the colored ribbon trace representing MC1R in magenta, MC3R in cyan, and MC5R in yellow.

pocket, similar to Arg8 of SHU9119. These results support the hypothesis that the high affinity of HS024 is due to involvement of Arg4 in charge-charge interactions with acidic residues on the opposite side of the hydrophobic region.

DISCUSSION

The cyclic peptides SHU9119, JKC363, HS014, and HS024 are known as potent antagonists of the melanocortin receptors. While SHU9119 is a nonselective antagonist, JKC363, HS014, and HS024 are selective antagonists of MC4R. The peptide HS014 is potent, selective for the MC4R ligand (K_i = 3.2 nM), and has 17-fold selectivity for MC4R over MC3R. The peptide JKC363 is three times more potent than HS014 for MC4R. The peptide HS024 has about 20-fold selectivity and very high affinity for MC4R (Chai et al., 2003; Kask et al., 1998). The ring of SHU9119 is formed through a lactam bond between lysine and aspartate residues, whereas JKC363, HS014, and HS024 employ a disulfide bond between two cysteine residues. The sizes of these macrocycles differ by three or six bond lengths, equivalent to the length of one or two amino acids. This could induce conformational change and influence the affinity or the selectivity of the ligand. A type I β-turn has been suggested as advantageous in binding melanocortin receptors (Li et al., 1999). However, the turn type is not a major determinant for receptor binding. This report shows that HS024 has high affinity for MC4R even with its distinctive turn conformation. When the solution structures of JKC363, HS014, and HS024 were compared with SHU9119, the orientation of Arg8 was found to be opposite between these two groups of peptides, and the backbone shape of the three peptides differed from SHU9119. However, three MC4R-selective peptides had electron distribution in the aromatic ring of *D*Nal6 that interacted with the positively charged Arg8 sidechain (Dougherty, 1996). Interactions between aromatic and charged residues have been reported to contribute to protein stability, based on the interaction between a protonated histidine residue and a neighboring tryptophan (Fernandez-Recio et al., 1997).

Based on our model of MSH-antagonist/MCR complex, we propose the following rules for receptor binding. The spatial orientation of the aromatic groups is more important than the charge-charge interactions between the positively charged Arg8 and the acidic residues in TMH2 and TMH3. However, the model of HS024/MC4R (Fig. 6B) shows that charge-charge interactions increase the binding affinity of the peptide for the MCR. This report describes the MC4R-selectivity of JKC363, HS014, and HS024 based on the unique interactions between the positively charged His264 sidechain of MC4R and the electron distribution in the aromatic ring of Trp9. Through MD simulations for MCRs, we found that MC4R has the sidechain of His264 situated inside the binding pocket of MC4R (Fig. 6C). Thus, when the three MC4R-selective cyclic peptides JKC363, HS014, and HS024 are docked into MC4R, they are stabilized by the interaction between Trp9 of the peptides and His264 of MC4R. A mutation study of His264 found that mutation affects the binding affinity for MC4R because His264 of MC4R interacts with the Ser121 of agouti signaling protein (ASIP), but mutation does not affect the binding affinity for MC1R (Chai et al., 2005). The histidine residue may be involved in hydrogen bonds, charge-charge interactions, and aromatic or charged residue interactions. We propose that His264 of MC4R acts as acceptor and Ser121 of ASIP acts as donor. This result supports our hypothesis that His264 of MC4R is involved in the interaction that stabilizes MC4R-selective antagonists bound to MC4R.

This report suggests a few structural features about selectivity for MC4R. As data accumulate about the structure-activity relationships of potent and selective novel ligands, we can use this information to improve the ligand for drug development.

ACKNOWLEDGMENTS

The World Class University program through the National Research Foundation of Korea funded by the Ministry of Education, Science and Technology (R33-2009-000-10123-0) supported this research. This research was partially supported by a Brain Korea (BK) project. We would like to thank Professor Kurt Wüthrich for fruitful discussion.

REFERENCES

Butler, A.A., Kesterson, R.A., Khong, K., Cullen, M.J., Pelleymounter, M.A., Dekoning, J., Baetscher, M., and Cone, R.D. (2000). A

unique metabolic syndrome causes obesity in the melanocortin-3 receptor-deficient mouse. Endocrinology *141*, 3518-3521.

Chai, B.X., Neubig, R.R., Millhauser, G.L., Thompson, D.A., Jackson, P.J., Barsh, G.S., Dickinson, C.J., Li, J.Y., Lai, Y.M., and Gantz, I. (2003). Inverse agonist activity of agouti and agouti-related protein. Peptides *24*, 603-609.

Chai, B.X., Pogozheva, I.D., Lai, Y.M., Li, J.Y., Neubig, R.R., Mosberg, H.I., Gantz, I. (2005). Receptor-antagonist interactions in the complexes of agouti and agouti-related protein with human melanocortin 1 and 4 receptors. Biochemistry *44*, 3418-3431.

Chen, A.S., Marsh, D.J., Trumbauer, M.E., Frazier, E.G., Guan, X.M., Yu, H., Rosenblum, C.I., Vongs, A., Feng, Y., Cao, L., et al. (2000). Inactivation of the mouse melanocortin-3 receptor results in increased fat mass and reduced lean body mass. Nat. Genet. *26*, 97-102.

Dougherty, D.A. (1996). Cation-pi interactions in chemistry and biology: a new view of benzene, Phe, Tyr, and Trp. Science *271*, 163-168.

Fan, W., Boston, B.A., Kesterson, R.A., Hruby, V.J., and Cone, R.D. (1997). Role of melanocortinergic neurons in feeding and the agouti obesity syndrome. Nature *385*, 165-168.

Fernandez-Recio, J., Vazquez, A., Civera, C., Sevilla, P., and Sancho, J. (1997). The tryptophan/histidine interaction in alpha-helices. J. Mol. Biol. *267*, 184-197.

Goodsell, D.S., Morris, G.M., and Olson, A.J. (1996). Automated docking of flexible ligands: applications of AutoDock. J. Mol. Recognit. *9*, 1-5.

Haskell-Luevano, C., Sawyer, T.K., Trumpp-Kallmeyer, S., Bikker, J.A., Humblet, C., Gantz, I., and Hruby, V.J. (1996). Three-dimensional molecular models of the hMC1R melanocortin receptor: complexes with melanotropin peptide agonists. Drug Des. Discov. *14*, 197-211.

Huszar, D., Lynch, C.A., Fairchild-Huntress, V., Dunmore, J.H., Fang, Q., Berkemeier, L.R., Gu, W., Kesterson, R.A., Boston, B.A., Cone, R.D., et al. (1997). Targeted disruption of the melanocortin-4 receptor results in obesity in mice. Cell *88*, 131-141.

Kask, A., Mutulis, F., Muceniece, R., Pahkla, R., Mutule, I., Wikberg, J.E., Rago, L., and Schioth, H.B. (1998). Discovery of a novel superpotent and selective melanocortin-4 receptor antagonist (HS024): evaluation *in vitro* and *in vivo*. Endocrinology *139*, 5006-5014.

Kollman, P. (1993). Free energy calculations: applications to chemical and biochemical phenomena. Chem. Rev. *93*, 2395-2417.

Lee, J.H., Lim, S.K., Huh, S.H., Lee, D., and Lee, W. (1998). Solution structures of the melanocyte-stimulating hormones by two-dimensional NMR spectroscopy and dynamical simulated-annealing calculations. Eur. J. Biochem. *257*, 31-40.

Lee, J.Y., Lee, S.A., Kim, J.K., Chae, C.B., and Kim, Y. (2009). Interaction models of substrate peptides and beta-secretase studied by NMR spectroscopy and molecular dynamics simulation. Mol. Cells *27*, 651-656.

Lewis, P.N., Momany, F.A., and Scheraga, H.A. (1973). Chain reversals in proteins. Biochim. Biophys. Acta *303*, 211-229.

Li, S.Z., Lee, J.H., Lee, W., Yoon, C.J., Baik, J.H., and Lim, S.K. (1999). Type I beta-turn conformation is important for biological activity of the melanocyte-stimulating hormone analogues. Eur. J. Biochem. *265*, 430-440.

Lindahl, E., Hess, B.A., and van der Spoel, D. (2001). A package for molecular simulation and trajectory analysis. J. Mol. Mod. *7*, 306-317.

Mountjoy, K.G., Robbins, L.S., Mortrud, M.T., and Cone, R.D. (1992). The cloning of a family of genes that encode the melanocortin receptors. Science *257*, 1248-1251.

Wessells, H., Hruby, V.J., Hackett, J., Han, G., Balse-Srinivasan, P., and Vanderah, T.W. (2003). Ac-Nle-c[Asp-His-DPhe-Arg-Trp-Lys]-NH2 induces penile erection via brain and spinal melanocortin receptors. Neuroscience *118*, 755-762.

Wuthrich, K. (1996). NMR structures of biological macromolecules. In Encyclopedia of Nuclear Magnetic Resonance, D.M. Grant, and R.K. Harris, eds. (New York, USA: Wiley), pp. 710-719.

Ying, J., Kover, K.E., Gu, X., Han, G., Trivedi, D.B., Kavarana, M.J., and Hruby, V.J. (2003). Solution structures of cyclic melanocortin agonists and antagonists by NMR. Biopolymers *71*, 696-716.